CFD Simulation of Heanched Heat Transfer in Concentric Tube with Inner Twisted Tape Insert By Using Nano Fluids

[1]J. Balabhaskara Rao, [2]D. Bhanuchandrarao, M. Ashok chakravarthy[3], K. Srinivasarao[4]
[1]*Associate Professor, Mechanical Engineering Department, Vaishnavi Engg.College, Srikakulam*[1]
[2]*M.Tech Student, Thermal engineering, V.R Siddhartha Engineering College, JNTU*
[3]*Assistant Professor, Mechanical Engineering, V.R Siddhartha Engineering College, JNTU*
[4]Asst. Professor, Mechanical Engineering Department, Vaishnavi Engg.College, Srikakulam[4]

***Abstract*— Heat transfer for heating and cooling fluids play an important role in many industries. The past literature reporting heat transfer enhancement techniques in different processes are abundant. Most of these enhancing techniques are based on flow geometry parameters (like fins arrangement or inserts) and/or improving the thermal properties of fluids. Conventional heat transfer fluids such as water, ethylene glycol (EG), propylene glycol (PG) and engine oil have inherently low thermal properties relative to nanofluids such as CuO, Al_2O_3 and TiO_2 fluids. Further increment the heat transfer rate of plane tube by inserting the twisted tape.**

The present project is CFD simulation analysis for thermal-hydraulic characteristics of CuO+(30%PG+70%water) different concentration (0.025% and 0.1% CuO) nanofluids flow inside a circular tube and with inserts. For the heat transfer in a circular tube fitted with twisted tape inserts, the parameters are pitch to inlet diameter ratio H/D=10 and H/D=5 spacer in laminar and turbulence flow conditions has been explained in this thesis using ansys fluent 6.2.3 taken up for the estimation of heat transfer enhancement of nanofluids at different volume concentrations under laminar and turbulent flow Reynolds number at constant heat flux boundary condition.

1 INTRODUCTION

Heat transfer enhancement is the process of improving the performance of a heat transfer system by increasing the heat transfer coefficient. In the past decades, heat transfer enhancement technology has been developed and widely applied to heat exchanger applications; for example, refrigeration, automotives, process industry, chemical industry etc. The performance of conventional Heat transfer fluids such as water, oils, ethylene glycol and propylene glycol are often limited by their low thermal conductivities.

Overcome these limitations some techniques have been developed for heat transfer enhancements over the years either to accommodate high heat fluxes in the limited area available or to reduce the size and consequently the cost in order to compete in the global market. Heat transfer enhancement is associated using external energy on the fluid through forced flow vibration / jet impingement and the use of electrostatic fields.

2 LITERATURE SURVEY

2.1 MAJOR CONTRIBUTORS

A number of experimental studies have been performed to investigate the transport properties of nanofluids, Eastman et al.(1997), Wang et al.(1999), Lee et al.(1999) and Xuan and Li (2000). These studies are concentrated on the evaluation of effective thermal conductivity under macroscopically stationary conditions. Limited studies on other aspects related to nanofluids such as phase change behavior has been due to Das et al.(2003), Tsai et al.(2003), You et al.(2003) and Vassallo et al.(2004).

Heris et al. [2006] conducted experiments in the laminar range with Al_2O_3 and CuO nanofluids and observed Al_2O_3 nanofluid to have higher heat transfer rates compared to CuO nanofluids.

Dittus – Boelter [1930], Gnielinski [1976], Tam and Ghajar [2006] and Churchill and Usagi [1972] developed correlations for estimation of heat transfer coefficient of single-phase fluid flow in a circular tube under fully developed and transitional flow conditions under constant heat flux boundary condition.

Xuan and Li [2003] estimated convective heat transfer coefficient of water+Cu nanofluid and found substantial heat transfer enhancement. At a Reynolds number of 20,000, the heat transfer coefficient containing 2% volume concentration of Cu nanoparticles in water is shown to be approximately 60% higher than that of pure water.

Single phase heat transfer enhancement with twisted tape inserts under laminar and turbulent flow conditions have been dealt by Smithberg and Landis [1964], Sarma et al. [2002] and with longitudinal strip inserts by Heish and Huang (2000), Saha and Langille [2002]. Experiments with nanofluids for heat transfer enhancements using twisted tape

inserts or longitudinal tapes have not been reported in literature.

Maiga et al. (2005) in this paper, we have investigated, by numerical simulation the hydrodynamic and thermal characteristics of a laminar forced convection flow of nanofluids inside (a) a straight heated tube and (b) a radial space between coaxial and heated disks. Two particular nanofluids were considered, namely Ethylene Glycol–cAl_2O_3 and water–cAl_2O_3. Results have clearly revealed that the addition of nanoparticles has produced a remarkable increase of the heat transfer with respect to that of the base liquids.

Sarma et al. [2008] have developed a correlation for the estimation of eddy diffusivity; Nusselt number of Al_2O_3 and CuO nanofluid in turbulent flow based on the experimental data published by various authors.

Bergman [2009] have been investigated the convective heat transfer coefficient of nanofluid under laminar flow condition and found that obtained specific heat of nanofluid is less compared to the specific heat of base fluid under same flow condition.

Sarma et al. [2002] making use of the equation of Smithberg and Landis [1964] for friction factor for flow in tubes under swirl flow observed that the classical equation of Van Driest for eddy diffusivity can be used successfully, if the coefficient in the equation is considered as a function of Reynolds number and twist ratio. They showed the variation of universal constant K for different twist ratios. Sarma et al. [2003] extended the analysis in the laminar flow range using the data of Kishore [2001] for friction factor obtained with Turbinol, thus encompassing a wide range of Reynolds and Prandtl number and also theoretically analyzed the convective heat transfer and friction factor of single phase fluid in plain tube with twisted tape inserts under laminar flow condition.

Sarma et al. [2005] theoretically developed a combined approach to predict the heat transfer and friction factor of single phase fluid in plain tube with twisted tape inserts at wide range of Reynolds number and Prandtl number.

Kumar and Prasad [2000] investigated the heat transfer and friction factor of water in solar water heating system with twisted tape inserts and found appreciable enhancement with inserts.

Klaczak [2001] presented experimental values of heat transfer enhancements with twisted tape insert in both in vertical and horizontal pipe at low Reynolds number range.

Saha and Dutta [2001] have been studied heat transfer and friction factor in circular tube by considering the uniform pitch, varying pitch and spacing between the pitch of twisted tape inserts.

2.2 SCOPE OF THE PRESENT WORK

It is observed from the literature that the experimental data for different nanofluids with twisted tape insert in laminar and turbulent flow conditions are available. However, no cfd simulation results are available for different volume concentrations of nanofluid in laminar to turbulent flow conditions with and without twisted inserts. The present aim is to estimate the heat transfer coefficient and friction factor of nanofluid in laminar to turbulent flow conditions in plain tube with and without inserts.

Heat transfer and friction factor of nanofluid in circular tube at low volume concentrations under the Reynolds number ranging from 500<Re<50000 at constant heat flux condition is estimated by using cfd simulation and the results are compared with the available literature and theory is developed.

The heat transfer coefficient and friction factor of different volume concentration of nanofluid and with twisted and insert (Twist ratios, H/D = 5 and10)..

2.3 PRESENT INVESTIGATION

CFD simulation analysis and Estimation of thermo-physical properties in addition of additives of CuO nano particle in base fluid in the volume concentrations of 0.025% and 0.1% is taken and heat transfer coefficient and friction factor of CuO nanofluid at Reynolds number range of 500 to 50,000 subjected to constant heat flux boundary condition. Heat transfer enhancements are Estimation with displaced enhancement devices like twisted tape inserts in tube at that Reynolds numbers.

3 ESTIMATE THE PROPERTIES OF NANOFLUID

3.1 INTRODUCTION

Thermo physical properties of nanofluid are essential for the evaluation of heat transfer coefficient. These roperties vary with concentration and temperature. The effect of variation of these parameters on thermo physical properties has been dealt by Lee et al. [1998], Das et al. [2000], Xuan and Roetzel [2003], Pak and Cho [1998] and Choi et al. [2003].

Thermo physical properties of base fluid (30% propylene glycol + water) are taken form ASHRAE HAND BOOK [1972]. These properties are given in table 3.1.

Table 3.1 Thermo-physical properties of base fluid from ASHRAE hand book.

3.2 VOLUME CONCENTRATION ESTIMATION

The quantity of copper oxide W_a to be added for different volume concentrations can be estimated from the relation

$$\% \text{ volume concentration} = \frac{\frac{W_a}{\rho_a}}{\frac{W_a}{\rho_a} + \frac{W_w}{\rho_w}} \qquad [3.1]$$

Where

ρ_a Density of alumina, 6310 kg/m^3

ρ_w Density of water, kg/m^3

W_w Weight of sample water says 100 grams

3.3 EVALUATION OF PROPERTIES

The thermo-physical properties of nanofluid like density, thermal conductivity, absolute viscosity, and specific heat are estimated with equations available in literature.

3.3.1 Density

Density of different volume concentrations of nanofluid is estimated by using Hydrometer and compared with the values of Pak and Cho [1998]. Density at different temperatures is estimated by Pak and Cho [1998] has given a regression formula.

$$\rho_{nf} = \phi \rho_p + (1-\phi)\rho_w \qquad [3.2]$$

Table: 3.1 Comparison of density with Pak and Cho [1998]

Sl.No.	Volume fraction, φ , (%)	Pak and Cho [1998]
1	0.025	1027
2	0.1	1031
3	0.4	1047
4	0.8	1068
5	1.2	1089

3.3.2 Thermal conductivity

Wasp [1977] proposed a thermal conductivity correlation in terms of nanoparticle volume concentration in the base fluid, which is given by

$$Knf = Kw\left[\frac{Kp + 2Kw - 2\varphi(Kw - Kp)}{Kp + 2Kw + \varphi(Kw - Kp)}\right]$$

[3.3]

Where, Kp, Knf, Kw are the thermal conductivity coefficients for the dispersed phase, mixture phase and continuous phase of the fluid and φ is volume concentration in percentage. Kc is the thermal conductivity of the base fluid at some reference temperature.

Table 3.2 Thermal conductivity of CuO nanofluid from wasp equation in literature

3.3.3 Absolute viscosity

Einstein [14] has proposed a viscosity correlation in terms of nanoparticle concentration in the base fluid, when the nanoparticle volume concentration is lower than 5%, which is given by

$$\mu_s = \mu_{bf}\left(1 + \frac{5}{2}\phi\right) \qquad (3.4)$$

The Einstein correlation is used to absolute viscosity calculation at different temperatures.

Table 3.3 shows the viscosity of CuO nanofluid with values of Einstein correlation

Temperature (^{o}k)	Density (kg/m3)	Thermal conductivity (w/m.k)	Viscosity (mPa-s)	Specific heat (j/kg.k)
273	1036.24	0.409	7.07	3.654548
283	1032.55	0.421	4.52	3.655633
293	1028.35	0.431	3.06	3.662165
303	1023.64	0.441	2.19	3.673319
313	1018.42	0.45	1.63	3.688373
323	1012.69	0.457	1.26	3.706677
333	1006.44	0.463	1.01	3.727682
343	99.69	0.469	0.83	3.750913
353	992.42	0.473	0.7	3.775986
363	984.65	0.476	0.6	3.802601
373	976.36	0.478	0.53	3.830547

S. No.	Volume fraction, φ , (%)	Viscosity of from Einstein, $\nu \times 10^{-6}$
1	0.025	2.5716
2	0.1	2.5765
3	0.4	2.5957
4	0.8	2.6214
5	1.2	2.7000

3.3.4 Specific heat

The specific heat of nanofluid is an important parameter that has to be evaluated theoretically. In this analysis nanofluid (nanoparticles + base fluid) is considered as homogeneous mixture. This formula is applied for the estimation of specific heat of nanofluid at different volume concentrations. The specific heat formula for homogeneous mixture is given by

$$C_{p_{nf}} = \frac{(m*Cp)_{CuO} + (m*Cp)_{bf}}{m_{CuO} + m_{bf}} \qquad [3.9]$$

The Cp of CuO is **760** J/kg K

S.No.	Volume fraction, φ , (%)	WaspModel [1977]
1	0.025	0.43632155
2	0.1	0.43632155
3	0.4	0.43632155
4	0.8	0.43632155
5	1.2	0.43632155

Table 3.4 shows the specific heat of CuO the values of homogeneous mixture formulae

S.No.	Volume fraction, φ, (%)	Specific heat from nanofluid
1	0.025	3666.3
2	0.1	3663.7
3	0.4	3650.5
4	0.8	3638.9
5	1.2	3624.8

All the thermo physical properties of different volume concentrations of nanofluid and at different temperature are estimated from the theoretical correlation are shown in the Table 3.6.

Table 3.5 thermo-physical properties different volume concentration nanofluid

S. No.	Volume fraction φ, (%)	Thermal conductivity (w/m.k)	Density (kg/m^3)	Viscosity (mpa-s)	Specific heat (j/kg.k)
1	0.025	0.43632155	1027	2.5716	3847.1
2	0.1	0.43632155	1031	2.5765	3844.3
3	0.4	0.43632155	1047	2.5957	3833.2
4	0.8	0.43632155	1068	2.6214	3818.2
5	1.2	0.43632155	1089	2.7000	3803.4

Table 3.6 thermo-physical properties 0.025% volume concentration nanofluid at different temperature

Temperature (^{o}k)	Thermal conductivity (w/m.k)	Density (kg/m3)	Viscosity (mPa-s)	Specific heat (j/kg.k)
273	0.40930196	1037.558	7.07441875	3.653665
283	0.42131067	1033.869	4.522825	3.654751
293	0.43131793	1029.67	3.0619125	3.661281
303	0.44132518	1024.962	2.19136875	3.672432
313	0.45033169	1019.743	1.63101875	3.687483
323	0.45733676	1014.014	1.2607875	3.705784
333	0.4633411	1007.766	1.01063125	3.726784
343	0.46934544	101.2426	0.83051875	3.750009
353	0.47334834	993.7494	0.7004375	3.775076
363	0.4763505	985.9813	0.600375	3.801685
373	0.47835195	977.6934	0.53033125	3.829624

Table 3.7 thermo-physical properties 0.1% volume concentration nanofluid at different temperature

Temperature (^{o}k)	Thermal conductivity (w/m.k)	Density (kg/m3)	Viscosity (mPa-s)	Specific heat (j/kg.k)
273	0.410209	1041.514	7.087675	3.651016
283	0.422244	1037.827	4.5313	3.652102
293	0.432273	1033.632	3.06765	3.658629
303	0.442302	1028.926	2.195475	3.669774
313	0.451328	1023.712	1.634075	3.684815
323	0.458348	1017.987	1.26315	3.703103
333	0.464365	1011.744	1.012525	3.724088
343	0.470383	105.9003	0.832075	3.747297
353	0.474394	997.7376	0.70175	3.772346
363	0.477403	989.9754	0.6015	3.798936
373	0.479409	981.6936	0.531325	3.826856

3.4 FINITE VOLUME METHOD

The mass, momentum, and scalar transport equations are integrated over all the fluid elements in a computational domain using CFD. The finite volume method is a particular finite differencing numerical technique, and is the most common method for calculating flow in CFD codes. This section describes the basic procedures involved in finite volume calculations.

The finite volume method involves first creating a system of algebraic equations through the process of discretising the governing equations for mass, momentum, and scalar transport. To account for flow fluctuations due to turbulence in this project, the RANS equations are discretised instead when the cases are run using the *k-epsilon* turbulence model. When the equations have been discretised using the appropriate differencing scheme for expressing the differential expressions in the integral equation (i.e. central, upwind, hybrid, or power-law, or other higher-order differencing schemes), the resulting algebraic equations are solved at each node of each cell.

3.6 SOLUTION TECHNIQUE

The value of the scalar properties of interest (i.e. temperature) at a particular location in the computational domain depends on the flow's direction and velocity, which must also be solved for in the calculation process. To There are many algorithms available for this purpose, the most popular are the SIMPLE and PISO methods. This section describes the SIMPLE algorithm and compares it to the PISO algorithm. In this project SIMPLE algorithm is used in calculation process.

PROBLEM DESCRIPTION AND MODELLING

5.1 Cfd Geometry Modeling

The geometry was making in catia (the CAD program). This geometry imported to ansys icem cfd and repairs the geometry. The geometry consist of a cylindrical tube of diameter 14.5 mm diameter and length of 2000 mm. The plain tube with helical twist configuration consists of a plain tube with above diameter and length, and a helical twist with twist ratio of 5 and 15 its lengths of 1700mm as shown in fig 5.1

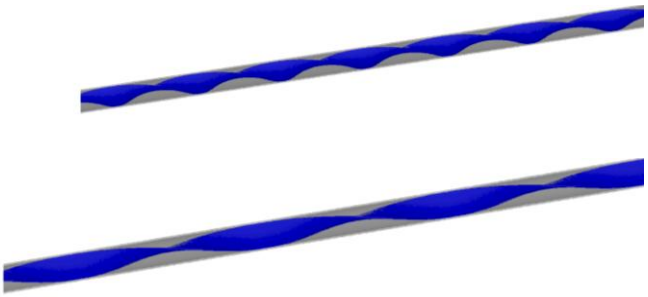

Fig 5.1 geometrical model of plane tube with twisted tape inserts

5.2 Grid Generation

The mesh has been generated in the Cartesian co-ordinate system. The grid independence test has been conducted and the grid has been refined in tube wall region. The generated grids are shown in Fig. 5.2.

The total number of cells in computational domain is **2, 12,480**.

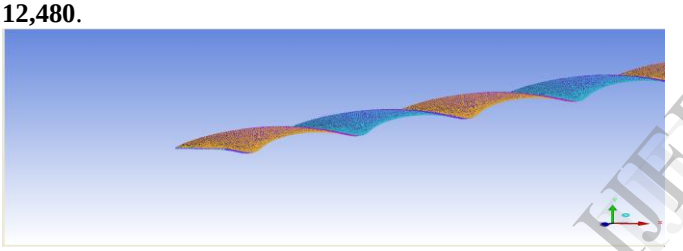

Fig 5.2. Grid for the twisted tape insert

5.3 Modeling parameters or Boundary Conditions

Boundary conditions are used in the simulations are as shown in fig 5.3 and different inlet velocities are shown in table 5.1

Table 5.1 Numerical values of the parameters used for simulation

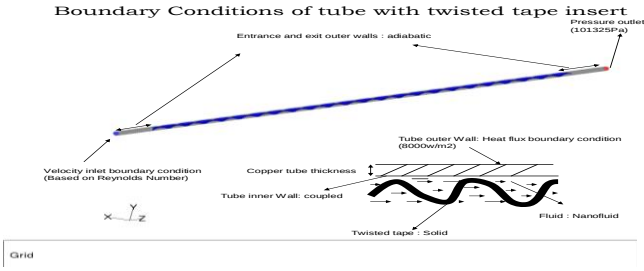

Fig 5.3 Boundary conditions of plane tube with twisted inserts

Heat flux	:	8340	W/m^2
Pressure outlet	:	101325	Pa
Inlet tempter	:	303	K
Fluid viscosity Base fluid	:	2.19	mPa-s
Nanofluid at 0.025%CuO concentration:		2.1914	mPa-s
Nanofluid at 0.025%CuO concentration:		2.1955	mPa-s
Fluid thermal conductivityBase fluid:		0.441	W/mK
Nanofluid at 0.025%CuO concentration:		0.4413	W/mK
Nanofluid at 0.025%CuO concentration:		0.4423	W/mK
Fluid densityBase fluid	:	1023.6	Kg/m^3
Nanofluid at 0.025%CuO concentration:		1025.3	Kg/m^3
Nanofluid at 0.025%CuO concentration:		1028.9	Kg/m^3
Fluids specific heat Base fluid:		3.6733	KW/KgK
Nanofluid at 0.025%CuO concentration:		3.6724	KW/KgK
Nanofluid at 0.025%CuO concentration:		3.6698	KW/KgK

3.4 Relaxation

The following relaxation factors for the various variables have been considered:

P1 - pressure, linear relaxation (LINRLX) : 1.0

U1 - velocity vector in X-axis, false-time-step relaxation (FALSDT) : 0.1

V1 - velocity vector in Y-axis, false-time-step relaxation (FALSDT) : 0.1

W1- velocity vector in Z-axis, false-time-step relaxation (FALSDT) : 0.1

TEM1 - Temperature, false-time-step relaxation (FALSDT) : 1.0

The relaxation parameters of other variables have been kept as the default values.

3.5 Convergence

The convergence criteria considered in the present investigation included stabilization of variables at different monitoring points as well as the mass & energy balance. The number of iterations needed to get the convergence was 1000 and/or convergence factor is taken as 0.001.

5.6 Numerical procedure and computational methodology

The governing differential transport equations were converted to algebraic equations before being solved numerically. After the specification of the boundary condition, the solution control and the initialization of the solution have to be given before the iteration starts. The solution controls like the pressure velocity coupling and the discrimination of the different variables and the relaxation factors have to be specified. The solutions sequential algorithm (called the segregated solver) used in the numerical computation requires less memory that the coupled solver. Since we are using the segregated solver for our problem, the default under relaxation factors are used and the SIMPLE scheme for the pressure velocity coupling is used and the second discrimination is used for the momentum and the standard scheme is used for the pressure.

RESULT AND DISCURSIONS

The observations of CFD simulation results are discussed below for the given boundary conditions.

6.1 variation of pressure drop in plain tube with and with out twisted tape

Fig. 6.1 shows that the pressure drop in a plain tube with and without twisted insert along its length. By referring y to the fig 6.1 one can observe that the pressure drop increases along the length with decreasing the twist ratio and in table 6.1, 6.2 and 6.3 can observe that the pressure drop increases with volume concentration of nano particles.

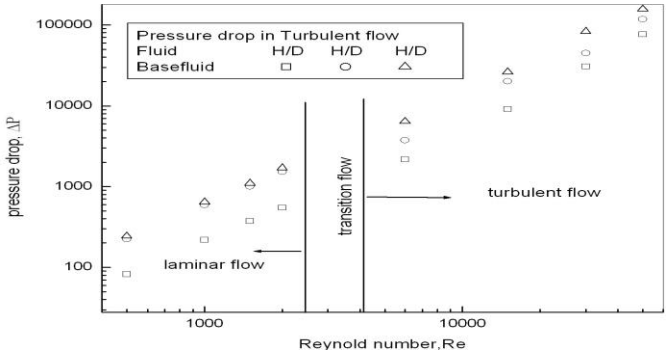

Fig 6.1 variation of pressure drop in plain tube with and with out twisted tape

6.2 Velocity distribution in plain tube with and with out twisted tape

Fig. 6.2 shows fluid flow pattern in a plain tube along its length. At the inlet of constant low temperature Nanofluid, the velocity of Nanofluid varies in the length direction. By referring to the Fig.1 one can observe that the inlet section the velocity profile can be change along the length unto sustain distance is called entrance length and remaining length the velocity profile doesn't change.

Fig. 6.3 and 6.4 shows that the fluids flow pattern in a plain tube with twisted insert along its length. By referring to the Fig.6.2 and 6.3 one can observe at the middle section of the velocity path lines the velocity is more at one side of twist and also observed that the maximum velocity of fluid flow decreases with increasing the twist ratio.

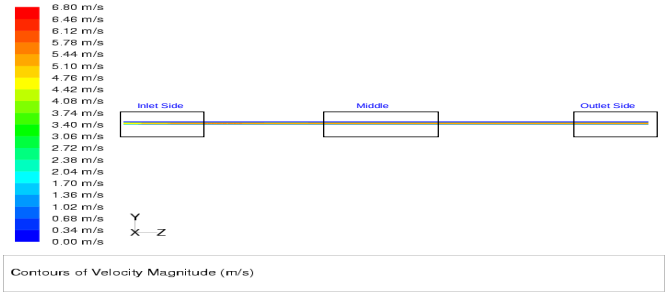

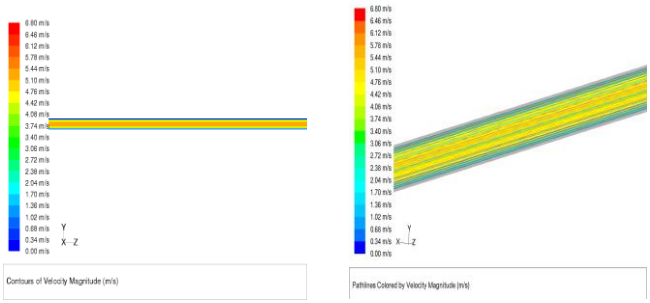

(a) At middle of plain tube

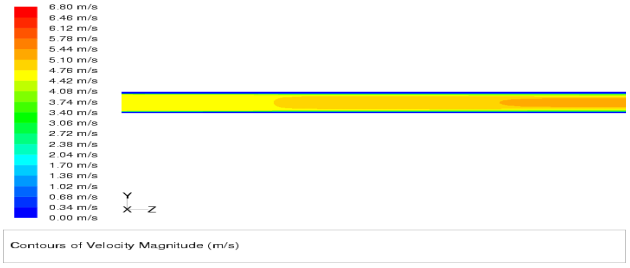

b) At the inlet of plain tube

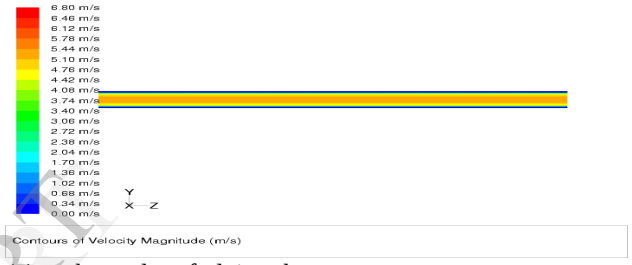

(c) at the outlet of plain tube

Fig 6.2 velocity magnitude and path lines of plane tube along the length at different sections

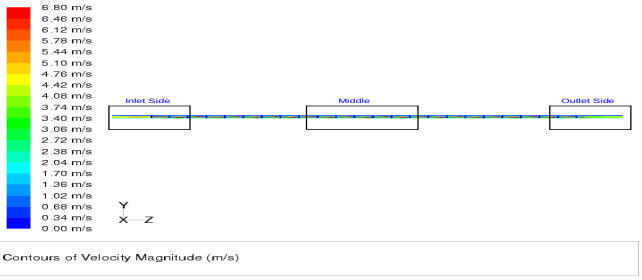

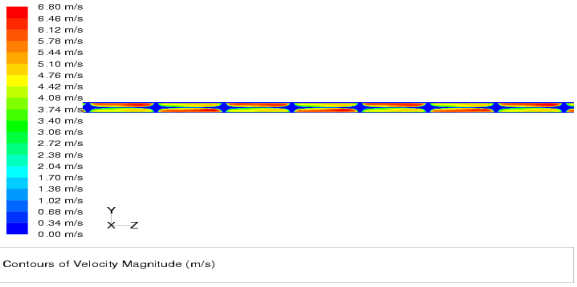

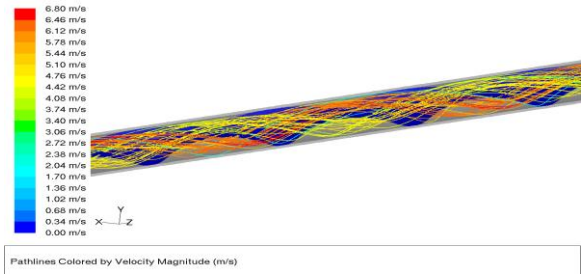

(a) At middle of plain tube

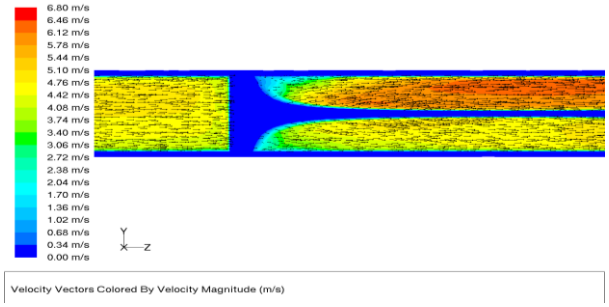

(b) At the inlet of plain tube

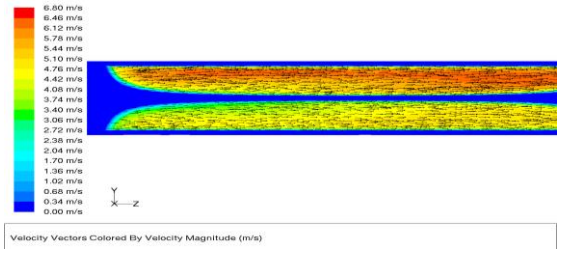

(c) at the outlet of plain tube

Fig 6.3 velocity magnitude and path lines of plane tube with insert H/D=5 along the length at different sections

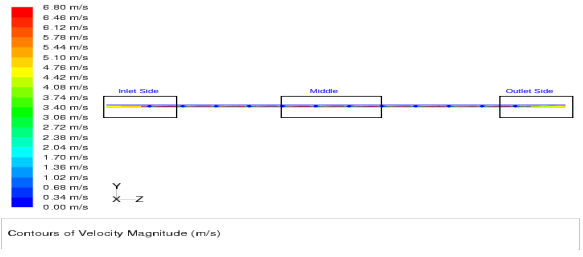

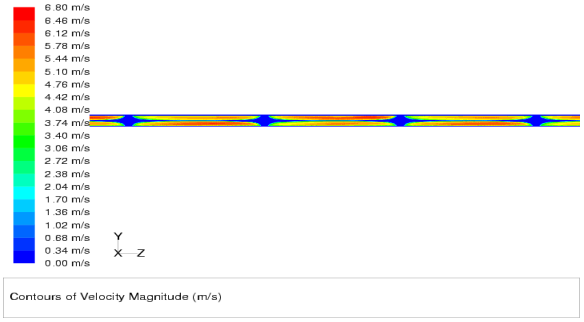

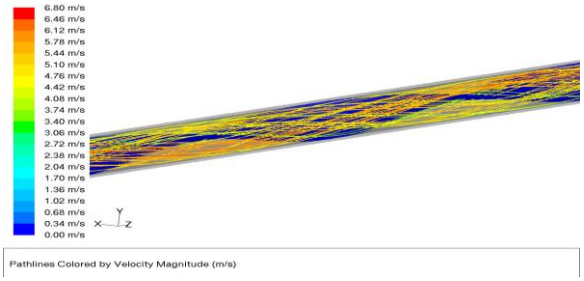

(a) At middle of plain tube

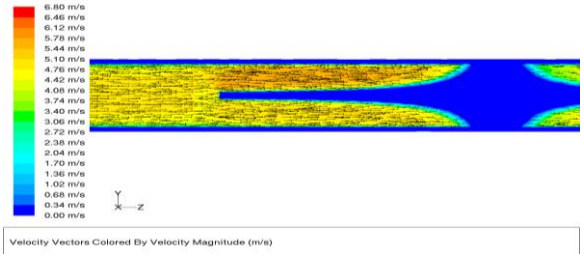

(b) At the inlet of plain tube

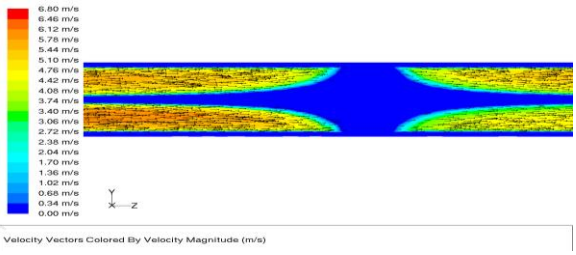

(d) at the outlet of plain tube

Fig 6.4 velocity magnitude and path lines of plane tube with insert H/D=10 along the length at different sections

6.3 friction factor and heat transfer enhancement in Plain tube

The results obtained in this simulation study are presented and discussed in this section. Figures show the variation of friction factor with Reynolds number for plain tube and the variation of heat transfer coefficient with Reynolds number for plain tube. By referring to the Figures one can observe that as Reynolds number increases heat transfer coefficient increases whereas friction factor decreases with Reynolds number and also can observe that increasing the volume concentration of CuO nano practical in the base fluid the heat transfer coefficient also increases.

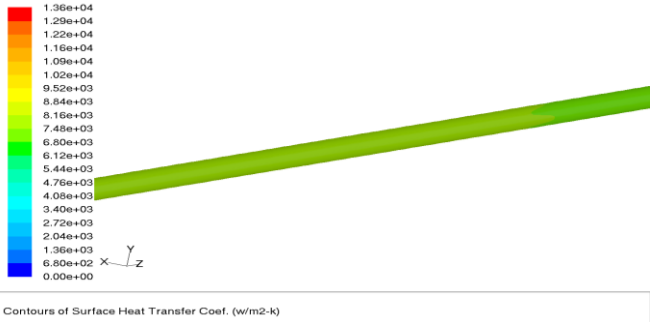

Fig 6.5 contours of surface heat transfer coefficient of plane tube

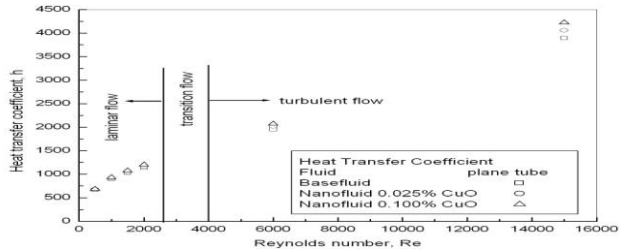

Fig 6.6 Comparison of heat transfer coefficient of base fluid and Nanofluid from simulation analysis of laminar and turbulent flows.

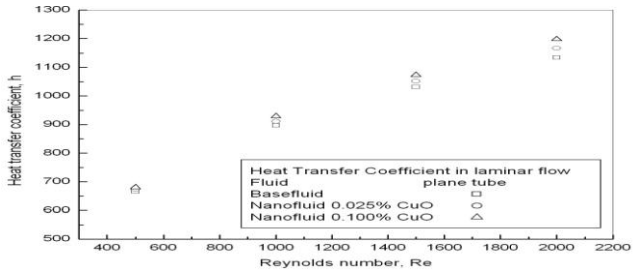

Fig 6.7 Comparison of heat transfer coefficient of base fluid and Nanofluid from simulation analysis of laminar flow

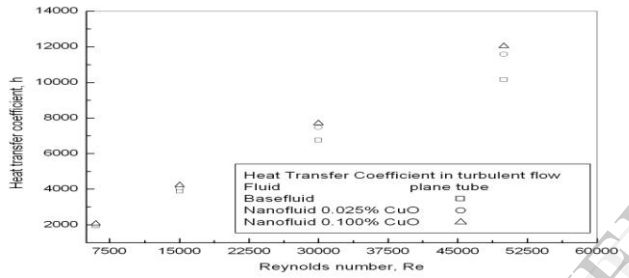

Fig 6.7 Comparison of heat transfer coefficient of base fluid and Nanofluid from simulation analysis of turbulent flow

6.4 Effect of twist on friction factor and heat transfer enhancement:

Variations of heat transfer coefficient with Reynolds number and Friction factor with Reynolds number for the tube fitted with regularly spaced twisted inserts are shown in Figures for twist ratio H/D =5 and H/D=10. Fig 6.8 and 6.9 as shown that heat transfer for a given Reynolds number increases with decreasing twist ratio indicating enhanced heat transfer coefficient due to enhanced swirl flow as the Reynolds number increases for given twist ratio. The Nusselt number also increases with Reynolds number indicating enhanced heat transfer coefficient due to increased convection as flow increases.

The data obtained by simulation are matching with the literature value for plain tube with the discrepancy of less than ± 15% for Nusselt number for Sharma et al [2002] and +8% for kishor [2005]) as shown in fig 6.10

Fig 6.8 contours of surface heat transfer coefficient of plane tube with twisted tape H/D=10

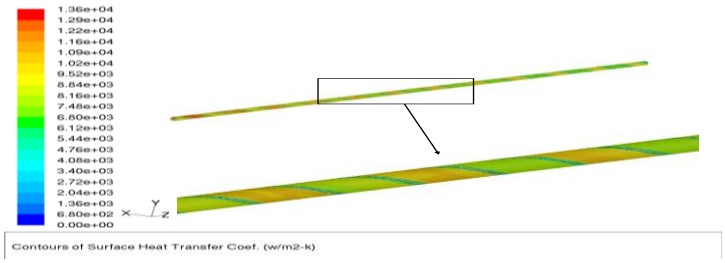

Fig 6.9 contours of surface heat transfer coefficient of plane tube with twisted tape H/D=5

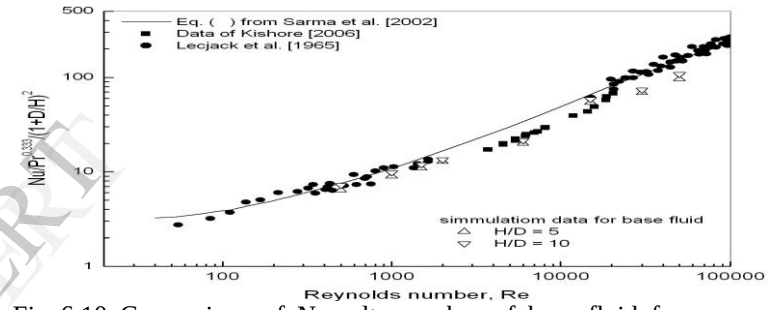

Fig 6.10 Comparison of Nusselts number of base fluid for literature in laminar and turbulent flow

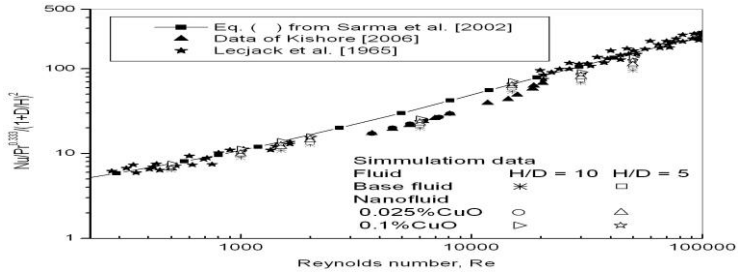

Fig 6.11 Comparison of Nusselts number of base fluid and Nanofluid for literature in laminar and turbulent flow

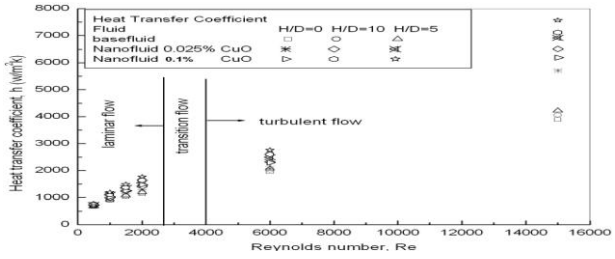

Fig 6.12 Comparison of heat transfer coefficient of base fluid and nano fluid for different twist ratios in laminar and turbulent flow

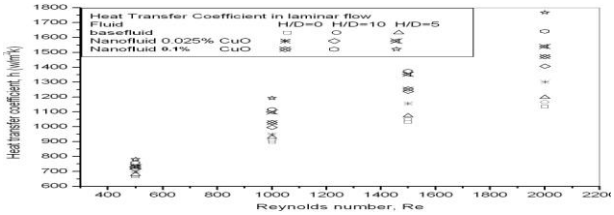

Fig 6.13 Comparison of heat transfer coefficient of base fluid and nano fluid for different twist ratios in laminar flow

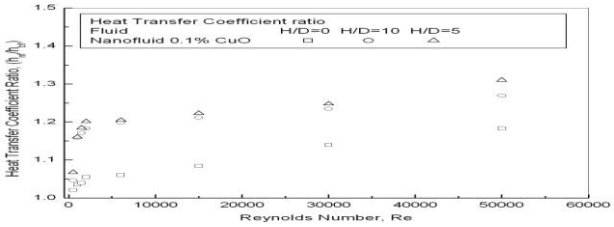

Fig 6.14 Comparison of heat transfer enhancement of 0.1% CuO nano fluid for different twist ratios in laminar and turbulent flow

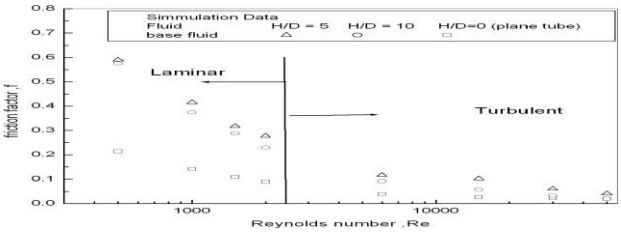

Fig 6.15 Comparison of friction factor of base fluid for different twist ratios in laminar and turbulent flow

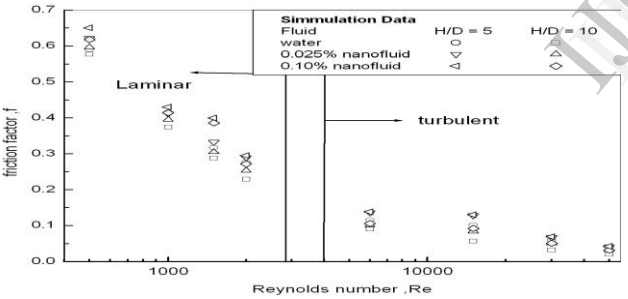

Fig 6.16 Comparison of friction factor of base fluid and nano fluids for different twist ratios in laminar and turbulent flow

CONCLUSIONS

CFD simulation for the heat transfer augmentation in a circular tube fitted with twisted inserts in laminar flow conditions with the Reynolds from has been explained in this paper using fluent version 6.2.16.

The data obtained by simulation are matching with the literature value for plain tube with the discrepancy of less than ± 15%.for Nusselt number and ± 10 % for friction factor. The simulated results for the tube fitted with twisted inserts are agreeing with the literature values ± 18% for Nusselt number and ± 15% for friction factor.

(1) From the simulation analysis 0.1% volume concentration CuO Nanofluid is having heat transfer enhancement of 17.16% compared to base fluid at 2000 Reynolds number.

(2) The heat transfer enhancement of CuO Nanofluid in plain tube with 0.1% volume concentration is 14.70% at 30000 Reynolds number and 19.12% at 50000 Reynolds number when compared to base fluid.

(3) Further heat transfer enhancement of 0.1% Nanofluid with twisted tape insert of H/D = 5 is having 26% at 30000 Reynolds number and 33. 2% at 50000 Reynolds number compared to the same fluid flowing in plain tube.

(4) The heat transfer enhancement of 0.1% Nanofluid with twisted tape insert of H/D = 5 is having 42.9% at Reynolds number 6000 and 86.01% at 50000 Reynolds number compared to base fluid flowing in a plain tube

REFERENCES

[1] S.K.Saha A.Dutta " Thermo hydraulic study of laminar swirl flow through a circular tube fitted with twisted tapes" Trans. ASME Journal of heat transfer June 2001, Vol-123/ pages 417-427.

[2] Zhi-Min Lin, Liang-Bi Wang "Convective heat transfer enhancement in a circular tube using twisted tape" Trans ASME journal of heat transfer Aug 2009,Vol-131/081901-1-12.

[3] Watcharin Noothong, Smith Eiamsa-ard and Pongjet Promvonge" Effect of twisted tape inserts on heat transfer in tube" 2nd joint international conference on "sustainable Energy and Environment 2006" Bangkok, Thiland.

[4] Paisarn Naphon "Heat transfer and pressure drop in the horizontal double pipes with and without twisted tape in-sert" 2005 Elsevier Ltd.

[5] Smith Eiamsa-ard , Chinaruk Thianpong, Pongjet Promvonge " Experimental investigation of heat transfer and flow friction in a Circular tube fitted with regularly spaced twisted tape elements" International Communications in Heat and Mass Transfer Vol. 33, Dec 2006.

[6] Ashis K. Mazumder, Sujoy K. Saha "Enhancement of Thermo hydraulic Performance of Turbulent Flow in Rec-tangular and Square Ribbed Ducts With Twisted-Tape Inserts" Journal of Heat Transfer AUGUST 2008, Vol. 130.

[7] A Dewan1 , P Mahanta1, K Sumithra Raju1 and P Suresh Kumar "Review of passive heat transfer augmentation